Catalysis Letters 1 (1988) 445–456

CO_2 CONVERSION AND OXALATE STABILITY ON ALKALI PROMOTED METAL SURFACES: SODIUM MODIFIED Al(100)

J. PAUL * and F.M. HOFFMANN

Corporate Research Science Laboratories, EXXON Research and Engineering Company, Route 22 East, Annandale, NJ 08801, U.S.A.

Received 12 August 1988; revised 31 October 1988

CO_2 conversion on alkali promoted metals in aprotic systems has been followed with surface sensitive spectroscopies. New results on sodium modified aluminum(100) are presented and compared with previous studies on magnesium [1], aluminum [2], and bulk alkali metals [3]. Electron energy loss spectra reveal two different states of CO_2 adsorption at 100 K and monolayer sodium coverage. Vibrational bands at 650 cm^{-1} and 2325 cm^{-1} correspond to weakly bound molecular CO_2 and a multitude of bands between 2300 cm^{-1} and 460 cm^{-1} to oxalate ions with low, possibly unidentate, coordination. Gentle annealing increases the coordination as apparent by vibrational shifts. This corresponds to oxalate to carbonate conversion, a process which is completed around room temperature. CO desorption was detected at 285 K and Auger measurements reveal a 1:3 C/O stoichiometry after high temperature annealing. We observe no release of CO_2 above 110 K but an additional weak state of CO desorption around 470 K. High temperature annealing causes decomposition of all intermediates and leaves the aluminum surface covered with an irreducible carbide and oxide overlayer. We suggest that CO_2 reduction and dimerization to $C_2O_4^{-2}$ is a common path to yield carbon deposition on all alkali promoted surfaces in hydrogen deficient systems. In contrast, oxalate decomposition is related to the specific chemistry of each substrate.

1. Introduction

The present communication relates to carbon dioxide conversion and the efficiency of carbon deposition in methanation catalysis. We argue that the lowered workfunction of an alkali promoted surface facilitates a high probability of electron transfer to impinging neutral CO_2 molecules. CO_2^- radicals react to oxalate ions, $C_2O_4^{2-}$, in hydrogen poor systems. Our results suggests that the dimerization occurs via a radical-substrate reaction rather than a radical-radical mechanism. The high probability for CO_2 reduction on promoted metal surfaces explain the observed two orders of magnitude higher efficiency of carbon deposition from CO_2 compared with from CO. The process of dimerization is a

* Present address: Department of Physics III, Royal Institute of Technology, S-100 44 Stockholm, Sweden.

general phenomenon in aprotic systems. The subsequent path of oxalate decomposition, in contrast, relates to the specific chemistry of the adsorbent. The decomposition has been demonstrated to be different on alkali promoted iron [4] and aluminum [this work] surfaces as well as on bulk polycrystalline alkali metals [3].

Carbon dioxide reduction is of interest in other branches of engineering science as well. Oxalate production through electrochemical reduction is a feasible, although not economically competitive process [5]. Of greater interest is the role of oxalate intermediates in potassium catalyzed CO_2 gasification reactions on carbon surfaces [6].

2. Experimental

Experiments were performed in an ultra high vacuum (UHV) chamber operated at 1×10^{-10} torr. The Al(100) crystal was cleaned following a documented 3 hr procedure [7]. Sodium was deposited from a SAES getter source. Carbon dioxide was dosed through a beamdoser. Gas doses are given in 'X L' Langmuirs ($1\ \mathrm{L} = 10^{-6}$ torrsec) as read on the ion gauge i.e. uncorrected for ion gauge sensitivity and beamdoser efficiency. The neglect of the ion gauge sensitivity will overestimate CO_2 doses by about 40% [8]. The beamdoser efficiency relative to backfilling was estimated to 50 : 1 for water [7]. We use typical exposure times of one minute. This means that a '1 L' exposure translates to an effective dose of 50 L at around 1×10^{-6} torr.

Electron energy loss (EEL) spectra were measured with a Leybold spectrometer ($E_k = 5$ eV, $R = 60\ \mathrm{cm}^{-1}$). Thermal desorption (TDS) traces were followed with the crystal in line of sight of the mass spectrometer (UTI 100C). The heating rate was 1.5 ksec^{-1}. The UTI manual postulates a m28/m44 ratio of 0.15 for CO_2 fragmentation and we measured 0.17 for the same ratio. Auger electron spectra (AES, $E_k = 3$ keV, $V_{pp} = 2$ V) were only measured prior to molecular adsorption or after decomposition of any molecular intermediate in order not to introduce any electron beam artefacts.

3. Results

3.1. ELECTRON ENERGY LOSS SPECTROSCOPY

Figure 1 shows EEL spectra for CO_2 adsorbed on Al(100) covered by a c(2 × 2) monolayer of sodium [9]. Exposure to CO_2 at 100 K gives rise to a multitude of peaks. Flashes to subsequently higher temperatures alter the vibrational structure first by surpressing the 650 cm^{-1} and 2325 cm^{-1} bands and later by shifting the double peak structure at 1310/1480 cm^{-1} to 1350/1570 cm^{-1}.

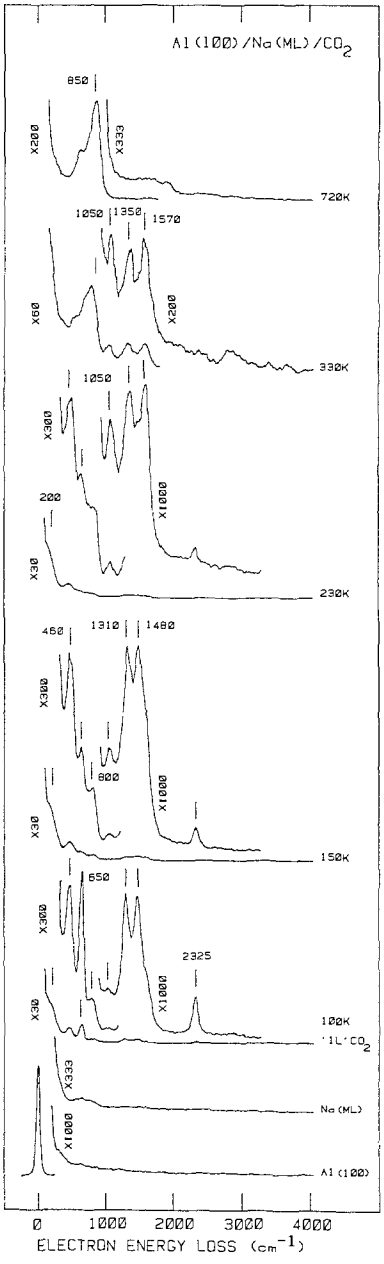

Fig. 1. Electron energy loss spectra of CO_2 adsorbed onto an annealed monolayer of sodium on Al(100). From below we display EEL spectra of (i) the clean Al(100) surface (ii) the annealed monolayer of sodium, (iii) Al(100)/Na(ML) after '1 L' of CO_2 at 100 K, and (iv) to (vii) flashed to increasingly higher temperatures. Analogous thermal desorption spectra are shown in fig. 2. Al(100)/Na(ML) is characterized by a c(2×2) $\theta = 0.50$ overlayer [9].

Table 1
Auger ratios after annealing to 700 K

Adsorption system	C272/0503	Stoichiometry C:O
Al/Na/CO	0.57 ± 0.04	1:1
Na(bulk on Al)/CO2	0.29 ± 0.03	1:2
Al/Na(ML)/CO2	0.19 ± 0.02	1:3

The 460 cm^{-1} band is correlated to the 1310/1480 cm^{-1} pair and the 1050 cm^{-1} band to the 1350/1570 cm^{-1} pair. Weak bands around 650, 800, and 2300 cm^{-1} also appear to be correlated to the 460/1310/1480 structure. Finally, spectra obtained after flashes to 720 K are dominated by vibrational structure around 850 cm^{-1}.

3.2. AUGER ELECTRON SPECTROSCOPY

EEL spectra revealed that no molecular intermediate survived annealing to above 470 K. At this temperature we observed the characteristic Auger peak profiles of aluminum oxide and aluminum carbide [9]. The relative intensities of the carbon 272 eV and oxygen 503 eV lines reveal a different ratio between carbide and oxide coverages after CO_2 decomposition on bulk sodium and aluminum modified by a monolayer of sodium [table 1]. The C272/0503 ratio after CO decomposition is given as a reference value [10]. This latter ratio is independent of alkali and CO coverages [11].

Previous surface titration measurements allow us to correlate AES intensities to surface coverages of Al_2O_3 and Al_4C_3 [9] and to evaluate the amount of deposited carbon per dosed gas equivalent [table 2]. The figures for the Auger ratio, C272/Al68, equal roughly the fraction of the surface covered by the carbide [9]. A relative efficiency factor was defined as the carbon Auger intensity, C272/Al68, devided by the gas dose, '*X* L'. We normalize the highest value to unity. Obviously this factor serves as a guidance rather than an absolute measurement of initial reaction probabililties.

Table 2
Carbon deposition efficiency

Substrate	Gas	Dose (100 K)	C272/Al68 (700 K)	Efficiency (arb. units)
K(bulk on Al)	CO	'50 L'	0.03	0.0002
Al/Na(ML)	CO	'200 L'	0.17	0.0003
Al/K(ML)	CO	'50 L'	0.2	0.001
Al/Na(ML)	CO_2	'1 L'	0.09	0.03
Na(bulk on Al)	CO_2	'1 L'	3.4	1

3.3. THERMAL DESORPTION SPECTROSCOPY

Figure 2 shows thermal desorption spectra of CO_3(m44), CO(m28), and Na(m23) from Al(100) modified by a monolayer of sodium and exposed to '1 L' of CO_2 at 100 K. Weakly bound molecular CO_2 desorbs at low temperature. The m44 peak saturates our measuring range but the contribution to the m28 intensity from the CO_2 cracking pattern is obvious around 110 K. We did not observe any CO_2 desorption at higher temperatures. Carbon monoxide desorption is observed at 285 K and 470 K. We also observe a higher sodium desorption temperature from the surface exposed to CO_2 than from the clean surface (fig. 2 and ref. [9]).

4. Discussion

4.1. IDENTIFICATION OF INTERMEDIATES

Weakly adsorbed molecular CO_2 was identified by its vibrational bands at 2325 cm^{-1} and 650 cm^{-1}. The close proximity of these frequencies to the dipole active

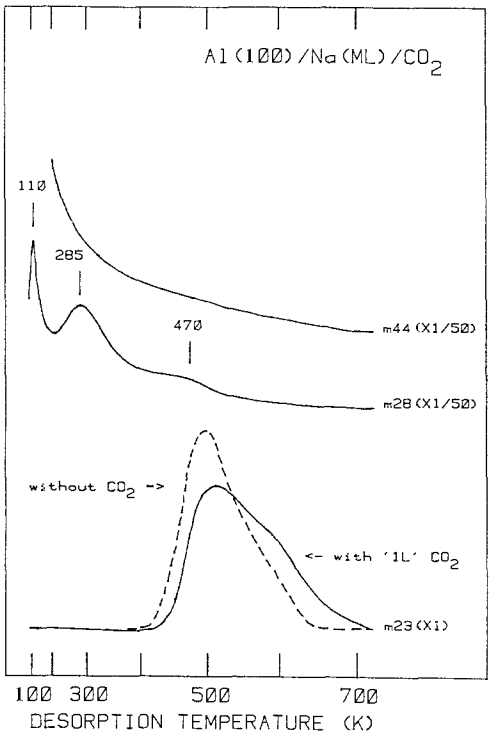

Fig. 2. Thermal desorption spectra after CO_2 adsorption ('1L'100 K) onto Al(100)/Na(ML, c(2×2)). The cracking pattern of CO_2 (m44) gives a 15% signal for CO (m28). Heating rate $\simeq$1.5 $ksec^{-1}$.

Table 3
Dominant IR absorption bands of some CO_2 related compounds

Substrate	Frequency (cm^{-1})	Ref.
Molecular carbon dioxide, CO_2		
gas phase	2349, 667	[22]
Na(bulk on Al)	2350, 650	[3]
Al(100)/Na(ML)	2325, 650	fig. 1
Fe(100)/K(ML)	2325, 650	[4]
CO_2^{-1}	1665	[23]
Oxalate ions, $C_2O_4^{-2}$: high coordination		
average	1700, 1400, 1250, 800	[12]
solid $Li_2C_2O_4$	1660, 1330, , 770,450	[24]
Na(bulk on Al)	1650, 1350, , 920	[3]
Fe(100)/K(ML)	1650, 1500, 1200, 800	[4]
Oxalate ions, $C_2O_4^{-2}$: low coordination		
$CO_2 \cdot CO_2^-$ (g, C_s)	2310, 1710, 1389, 1339, 771, 656, 642	[25]
Al(100)/Na(ML)	2300, , 1480, 1310, 800, 650, 460	fig. 1
Carbonate ions: basic salts		
solid Na_2CO_3	1440, , , 878,	[26]
solid K_2CO_3	1450, , , 865,	[26]
Fe(100) K(ML)	1450,	[4]
Na(bulk on Al)	1450, , 1100, , 300	[3]
Carbonate ions: A_1 modes, B_2 modes		
unidentate(Co)	1460, 1367, 1068, 756, 354	[27]
Ag(110)	1360, 1050, 850, 270	[13]
bidentate(Co)	1608, 1277, 1030, 760, 385	[27]
Al(100)/Na(ML)	1570, 1350, 1050,	fig. 1

modes of gas phase CO_2 suggests a weakly perturbed and neutral species (table 3). The 2325 cm^{-1} and 650 cm^{-1} peaks become less intense after low temperature annealing. This attenuation correlates with a maximum in the CO_2 partial pressure around 110 K (fig. 2). The combined TDS and EELS observations make it plausible to proclaim weak molecular adsorption states on promoted surfaces.

The following two intermediate states were characterized by their respective vibrational frequencies. At 150 K an intermediate species showed strong bands at 460, 1310, and 1480 cm^{-1} and weak bands around 650, 800, and 2300 cm^{-1}. A second, high temperature species at 330 K was dominated by strong bands at 1050, 1350, and 1570 cm^{-1}. The conversion of the '150 K' form to the '330 K' form was correlated to the release of carbon monoxide around 285 K. This occurred at a temperature previously identified as the oxalate to carbonate

conversion temperature of bulk alkali oxalate [3]. Hence, we try to identify the '150 K' and '330 K' forms with known oxalate and carbonate structures (table 3). CO_2 adsorption on a bulk sodium film gives vibrational frequencies which overlap those of $Li_2C_2O_4$ and other highly coordinated oxalate ions [3]. We know from table 2 that these data represent above unity carbon and oxygen coverage. Vibrational modes at 1650 cm^{-1}, 1350 cm^{-1}, and 920 cm^{-1} consequently represent a 3D film of bulk sodium oxalate. The term bulk compound is here synonymous with Nakamotos basic or mineral salt [12].

The vibrational fingerprint of the oxalate ions on an aluminum surface promoted by a single layer of sodium atoms is different from that of a bulk sodium film and also different from that of a modified iron substrate (table 3). This is not surprising considering the span of oxalate vibrational frequencies of bulk compounds. The 'average' numbers quoted in table 3 bear considerable variations and Nakamoto discusses six principal ways of coordination [12]. The six ways are (i) unidentate, (ii) bidentate, and (iii–vi) bridging between 2–4 metal atoms. Whereas vibrational data for highly coordinated oxalate ions are abundant, data for unidentate species are not. Available data for CO_2 bound to the CO_2^- anion radical, however, agree well with observed frequencies (table 3). Consequently, we assign the '150 K' species as an oxalate species with low, possibly, unidentate coordination. It is mere semantics if one prefers to call this a strong binding site for CO_2 associated with adsorbed CO_2^- rather than an oxalate group. This explains the similarity between the 'oxalate bands' around 2300 cm^{-1} and 650 cm^{-1} and the corresponding bands of weakly adsorbed CO_2.

The '330 K' form was suggested to be a carbonate. Again we utilize literature data for the identification (table 3). The basic salt is characterized by a very strong band around 1450 cm^{-1} and much weaker bands around 1100 cm^{-1} and 850 cm^{-1}. Following the above discussion about oxalate formation we clearly observed the formation of a 3D carbonate for a bulk sodium film [3]. The strong 1450 cm^{-1} band following CO_2 adsorption on Fe(100) also suggested the formation of a highly coordinated carbonate group. A lower coordination than in the basic salt means a loss of degeneracy in the 1450 cm^{-1} band. This is observed as more structure rich spectra for unidentate and bidentate species (table 3). The coordination of the '330 K' species on Al(100)/Na(ML) is less straightforward because we cannot restrict ourselves only to totally symmetric modes. We suggest, however, that the high frequency of the 1570 cm^{-1} band indicate a carbonate bound to the substrate via two oxygen atoms. Moreover, the species must be tilted to explain the excitation of a B_2 mode, normally dipole forbidden according to 'surface selection rules'.

The band at 800/850 cm^{-1} is readily identified as an Al-O vibration (fig. 1). This band shifts to higher frequency as the 3D oxide develops and we recognize the familiar profile of aluminum oxide after annealing to 700 K [14]. The pure oxide shows a pronounced three peak structure which smoothens in the presence of hydroxyl groups or residual carbon [15]. Auger spectra clearly showed the

formation of aluminum carbide following high temperature annealing. Previously we assumed that the smoothened EELS profile of Al_2O_3 in the presence of Al_4C_3 was the result of superimposed spectra [10]. This assumption was most likely incorrect since we were unable to register any Al-C vibrational losses from a polycrystalline but oxygen free Al_4C_3 overlayer [J. Paul and F.M. Hoffmann, unpublished]. The smoothening must come from disorder in the Al_2O_3 lattice caused by the carbide rather than from the carbide itself. Finally, the shoulder on the elastic peak around 200 cm^{-1} corresponds to alkali-oxygen vibrations [16].

4.2. CARBON DIOXIDE CONVERSION

Oxalate ions form on different alkali promoted and hydrogen deficient surfaces exposed to carbon dioxide [3,4]. The process of oxalate formation is the predominant path to strong binding sites for CO_2 products on these surfaces. We suggest that carbon dioxide reduction is facilitated by electron transfer from the promoted surface followed by dimerization. The latter process could occur either via radical-substrate ($CO_2^- + CO_2 + e^-$) or radical-radical ($CO_2^- + CO_2^-$) reactions [5]. The observed monocoordinated oxalate species suggests the former mechanism.

CO_2 reduction to an anion is normally a slow reaction [5] but matrix isolation studies have shown that alkali metals and CO_2 readily form stable clusters, $Li^+CO_2^-$ etc. [17]. Annealing caused aggregation and oxalate was registered as the 'final' product [17]. Manceron et al. suggested a radical-substrate reaction for this dimerization [17]. Some support for this model may also be given by the measured low yields of dimerization of artificially produced CO_2^- anions, trapped in a potassium halide [18].

There are alternative ways to provide strong binding sites for CO_2 products. Carbonate formation through reaction with adsorbed oxygen atoms have been observed on silver [13] and XPS data suggest carbon dioxide dissociation followed by carbonate formation on unmodified polycrystalline aluminum surfaces [2] and single crystalline Mg(0001) surfaces [1]. The temperature and pressure dependences of CO_2 conversion on magnesium suggest the participation of a precursor dimer state, CO_2^--CO_2 [1], analogous to the oxalate state discussed in this communication. We have not observed any CO_2 adsorption on the clean Al(100) surface at LN_2 temperature (< 100 K) and exposures as outlined in section 2. We suggest that surface atoms with low coordination numbers and significantly higher pressures may explain the observed activity on a polycrystalline sample [2].

4.3. OXALATE DECOMPOSITION

The above discussed oxalate formation is largely a metal independent process promoted by alkali additives. The further path of oxalate decomposition is

instead closely linked to the carbon and oxygen stability on the specific metal. A thick overlayer of sodium oxalate converts to sodium carbonate around room temperature but the related release of CO is not observed for a bulk film in the presence of excess sodium metal [3]. Less than stoichiometric amounts of carbon monoxide is released because of sodium induced CO dissociation [3,10,11]. The bulk alkali carbonate lattice is stable to around 540 K when it decomposes to an oxide and gaseous CO_2 [19]. Carbon is thus deposited from CO dissociation following oxalate decomposition and additional oxygen from carbonate instability. These two effects give a 1:2 C/O stoichiometry for a bulk film after high temperature annealing (table 1). Carbon and oxygen will be present as a Al_2O_3/Al_4C_3 mixture on an aluminum substrate.

Annealing to around room temperature again converts oxalate groups to carbonate groups on Al(100) modified by a monolayer of sodium (fig. 1). This conversion is correlated to the simultaneous release of CO (fig. 2). A monolayer obviously cannot encapsulate CO following oxalate decomposition. The decomposition of the bicoordinated carbonate was, in contrast to the situation for basic salt, not correlated to CO_2 evolution. Carbonate instability and immediate release of CO during oxalate conversion lead to a 1:3 C/O stoichiometry after high temperature annealing.

The situation is different on a promoted iron surface. Again we observe the very efficient deposition of carbon through low temperature CO_2 reduction, dimerization, and oxalate formation [4]. The oxalate decomposes either to carbonate groups and CO around room temperature or further to adsorbed carbon monoxide and oxygen atoms. The simultaneous desorption of alkali atoms and CO molecules as well as CO_2 desorption around 570 K were detected. CO recombination, in comparison, occurs at 800 K on Fe(100).

5. Summary and conclusions

Utilizing surface sensitive spectroscopies we have observed CO_2 adsorption and conversion on alkali modified metal surfaces.

(i) Alkali promotion leads to CO_2 reduction. The electron transfer is facilitated by the reduced ionization potential of the promoted adsorbent. The anion radicals react to oxalate groups, $C_2O_4^{-2}$, probably through radical-substrate reactions. The dimerization occurs in aprotic systems and is metal independent.

(ii) The oxalate intermediates are stable to around room temperature on all surfaces. The decomposition is metal dependent and leads either to a carbonate and CO or directly to adsorbed oxygen and carbon atoms.

(iii) The adsorption probability of CO_2 increases with alkali coverage in contrast to the CO adsorption probability which decreases drastically. This leads to a two orders of magnitude higher efficiency for carbon deposition from CO_2 compared with from CO on promoted aluminum. Alkali metals promote reactive

adsorption of CO_2 on the overlayer and strong molecular adsorption of CO on the modified underlying substrate [4,20,21].

(iv) C-C bonds between the molecular adsorbents are clearly formed following CO_2 exposure on alkali promoted and hydrogen free surfaces. The corresponding formation of OC-CO bonds after CO exposure has yet to be proven. Coadsorption studies of CO_2 and hydrogen on alkali promoted surfaces are highly wanted.

Acknowledgements

We are greatful for many discussions with J.L. Robbins, Corporate Research, EXXON Research and Engineering Company. We also acknowledge the assistance of Jeff Seymour, Heyden & Son, London and Wayne Liss, Sadtler, Philadelphia in locating reference IR data for $Li_2C_2O_4$.

References

[1] S. Campbell, P. Hollins, E. McCash and M.W. Roberts, J. Electr. Spectr. Rel. Phen: 39 (1986) 145;
R.G. Copperthwaite, P.R. Davies, M.A. Morris, M.W. Roberts and R.A. Ryder, Cat. Lett. 1 (1988) 11.
[2] A.F. Carley, D.E. Gallagher and M.W. Roberts, Surf. Sci. 183 (1987) L263;
A.F. Carley, D.E. Gallagher and M.W. Roberts, Spectrochim. Acta 43A (1987) 1447.
[3] J. Paul, F.M. Hoffmann and J.L. Robbins, J. Phys. Chem. (in press).
[4] J. Paul, S.D. Cameron and D.J. Dwyer, (in preparation).
[5] E.M. Bennett, B.R. Eggins, J. McNeill and E.A. McMullan, Anal. Proc. (London) 17 (1980) 356;
C. Amatore and J.M. Saveant, J. Amer. Chem. Soc. 103 (1981) 5021;
T. Meisel, Z. Halmos, K. Seybold and E. Pungor, J. Thermal. Anal. 7 (1975) 73;
F. Solymosi, J. Kiss and I. Kovacs, J. Phys. Chem. (in press);
Catalytic Activation of Carbon Dioxide, ACS Symposium Series 363, ed. W.M. Ayers (ACS, Washington, 1988).
[6] S.R. Keleman and H. Freund, J. Cat. 102 (1986) 80.
[7] J. Paul and F.M. Hoffmann, J .Phys. Chem. 90 (1986) 5321.
[8] see e.g. L. Holland, J. Yarwood and W. Steckelmacher, *Vacuum Manual* (Halsted Press, New York, 1974).
[9] J. Paul, J. Vac. Sci. Technol. A 5 (1987) 664.
[10] J. Paul and F.M. Hoffmann, J. Chem. Phys. 86 (1987) 5188.
[11] J. Paul, Nature 323 (1986) 701.
[12] K. Nakamoto, *Infrared and Raman Spectra* (Wiley, New York, 1986) p. 245; and references therein.
[13] E.M. Stuve, R.J. Madix and B.A. Sexton, Chem. Phys. Lett. (1982) 89, 48.
[14] J.L. Erskine and R.L. Strong, Phys. Rev. B (1982) 25, 5547;
J.E. Crowell, J.G. Chen and J.T. Yates, Surf. Sci. (1986) 165; 37; ref. 7.
[15] J.E. Crowell, J.G. Chen and J.T. Yates, J. Electron. Spectr. Rel. Phenom. (19986) 39, 97; ref. 9.
[16] R.A. dePaola and F.M. Hoffmann, J. Chem. Phys. 87 (1987) 1361.

[17] L. Manceron, A. Loutellier and J.P. Perchard, J. Mol. Structure 129 (1985) 115.
[18] I.C. Hisatsune, T. Adl, E.C. Beahm and R.J. Kempf, J. Phys. Chem. 74 (1970) 3225; J.E. Bennett, S.C. Graham and B. Mile, Spectrochim. Acta 29A (1973) 375.
[19] H.P. Bonzel, G. Broden and H.J. Krebs, Appl. Surf. Sci. 16 (1983) 373.
[20] A. Berko and F. Solymosi, Surf. Sci. 171 (1986) L498.
[21] J. Paul and F.M. Hoffmann, Surf. Sci. (1988) 194; 419; J. Paul, Phys. Rev. B 37 (1988) 6164.
[22] G. Herzberg, *Molecular Spectra and Molecular Structure II. Infrared and Raman Spectra of Polyatomic Molecules* (Nostrand, New York, 1945) p. 272.
[23] K.O. Hartman and I.C. Hisatsune, J. Chem. Phys. 44 (1966) 1913.
[24] Sadtler Spectrum Y 996 K from The Matheson Company, East Rutherford, New Jersey, USA.
[25] S.H. Fleischman and K.D. Jordan, J. Phys. Chem. 91 (1987) 1300.
[26] F.A. Miller and C.H. Wilkins, Anal. Chem. 24 (1952) 1253.
[27] Unidentate and bidentate carbonates are represented by data for Cobalt compounds, ref. 12.